

Interferometric observations of R Leonis in the K band*

First direct detection of the photospheric pulsation and study of the atmospheric intensity distribution

G. Perrin¹, V. Coudé du Foresto¹, S.T. Ridgway², B. Mennesson¹, C. Ruilier¹, J.-M. Mariotti¹, W.A. Traub³, and M.G. Lacasse³

¹ Observatoire de Paris, DESPA, F-92195 Meudon, France

² National Optical Astronomy Observatories, Tucson, AZ 85726-6732, USA

³ Harvard-Smithsonian Center for Astrophysics, Cambridge, MA 02138, USA

Received 21 December 1998 / Accepted 2 February 1999

Abstract. The Mira-type star R Leonis was observed at two different epochs in the K band with the FLUOR beam combiner on the IOTA interferometer. A variation of diameter is clearly detected for the very first time at this wavelength revealing an apparent pulsation of atmospheric layers very close to the stellar photosphere. We discuss the excess of visibility measured at high spatial frequencies and show that they very likely reveal smaller diameters of the photosphere (22–24 mas) than those deduced on the basis of shorter frequency components. This smaller diameter makes R Leonis a fundamental pulsator. Mira models are compared to our data and a disagreement with spatial intensity distribution and dynamical behaviour is found.

Key words: techniques: interferometric – stars: fundamental parameters – stars: individual: R Leo – stars: AGB and post-AGB – infrared: stars

1. Introduction

Among all classes of variable stars, Mira-type stars may be distinguished as they play an important role in the enrichment of the interstellar medium with dust and gas through a mass loss process occurring on the Asymptotic Giant Branch. Pulsations of the central core induce large variations of brightness of Mira variables in the visible and smaller modulations of infrared magnitudes. Our Sun will enter the Mira phase at the twilight of its life. Because they are very luminous, cool and embedded in a dust shell that extends over several hundreds of solar radii, these stars are well suited to be studied with high angular resolution techniques at infrared wavelengths. The advantage of the K band for these observations is that it is close to the peak of

flux emitted by the star and that the opacity of the shell is lower than in the visible, allowing us to see deeper into the star.

One of the closest and most luminous Miras, R Leonis has been studied by many other groups using diverse high angular resolution techniques in the visible and near infrared domains. Speckle interferometric imaging in the visible showed a dependence of size with wavelength (Labeyrie et al. (1977)). The angular diameter of R Leonis has been determined at 2.16 μm by Di Giacomo et al. (1991) using the lunar occultation technique. Geometry dependence with wavelength was confirmed by multi-aperture observations in the visible (Tuthill et al. (1994), Haniff et al. (1995)). Using long baseline interferometry at 11.15 μm , Danchi et al. (1994) have observed the dust around R Leonis. Recently, Lattanzi et al. (1997) have studied R Leonis with the Fine Guidance Sensor of the Hubble Space Telescope as a visible interferometer and claim a detection of a 20% relative difference in size of the star along two orthogonal axes. The COAST interferometer has monitored the diameter of the star at visible wavelengths during three consecutive photospheric cycles and huge periodic variations of the diameter of some layers in the atmosphere have been detected (Burns et al. (1998)).

We present, in this paper, some new observations of the Mira-type star R Leonis in K at two different epochs in 1996 and 1997. These new data, complementary to those listed before, present evidence of time-dependent geometrical properties of the photosphere of the star. In Sect. 2, observations at the IOTA interferometer with the FLUOR beam combiner that have produced these data are presented. In Sect. 3, we study the intensity profile of R Leonis and diameters for the different periods are derived. We establish and discuss the variation of the diameter of the photosphere with visible phase in Sect. 4 and the corresponding effective temperatures are derived. The results in K on variability are compared to other evidence. In Sect. 5 we discuss the implications of the high frequency visibilities obtained in 1997 on the modeling of R Leonis. Finally, considerations for future observations are given in Sect. 6.

Send offprint requests to: G. Perrin (perrin@hplyot.obspm.fr)

* based on observations collected at the IOTA interferometer, Whipple Observatory, Mount Hopkins, Arizona.

Table 1. The observed data

Date (d/m/y)	mean JD −2450000	Visual phase	Projected baseline (m)	Azimuth (°)	Spatial frequency (arcsec ^{−1})	Visibility (%)
17/04/96	190	0.24	15.38	60.7	34.70	21.27 ± 0.35
17/04/96	190	0.24	14.26	80.3	32.18	27.23 ± 0.41
17/04/96	190	0.24	14.13	86.9	31.88	27.23 ± 0.40
17/04/96	190	0.24	14.13	92.5	31.88	27.18 ± 0.43
18/04/96	191	0.25	15.01	65.4	33.85	23.73 ± 0.33
03/03/97	510	0.27	32.37	63.10	73.02	07.70 ± 0.32
04/03/97	511	0.28	10.76	68.50	24.28	42.48 ± 0.36
04/03/97	511	0.28	10.30	86.00	23.24	45.56 ± 0.41
05/03/97	512	0.28	15.25	62.50	34.40	17.61 ± 0.71
06/03/97	513	0.28	15.19	63.20	34.27	16.56 ± 0.50
06/03/97	513	0.28	14.67	70.90	33.10	17.51 ± 0.29
06/03/97	513	0.28	14.38	77.00	32.43	19.34 ± 0.36
10/03/97	517	0.29	20.89	58.50	47.13	11.88 ± 0.60
10/03/97	517	0.29	19.57	71.20	44.15	12.55 ± 0.96

2. Observations

R Leonis was observed in 1996 and 1997 with the IOTA¹ interferometer located at the Smithsonian Institution’s Whipple Observatory on Mount Hopkins in Arizona. IOTA is a two element interferometer (a third telescope is under construction) operated both at visible and infrared wavelengths (Carleton et al. (1994), Traub (1998)). We have used the FLUOR² beam combiner to sample the spatial coherence of the sources. Progress reports on FLUOR have been presented at several conferences (see Perrin et al. (1996a), Perrin et al. (1996b), Coudé du Foresto et al. (1998)) and it will be described in more details in a forthcoming paper. The recombination is achieved in the photometric K band with single-mode fluoride glass fibers. The fibers filter out the wavefronts which are corrugated by atmospheric turbulence and trade phase fluctuations against photometric fluctuations which are monitored. It is then possible to directly calibrate and correct for the non-stationary atmospheric transfer function, alleviating severe inaccuracies in visibility calibrations which plague classical (multi-mode) beam combiners. The current accuracy on final visibility estimates with FLUOR is 1% for most sources and is as good as 0.3% on very bright sources.

The data are acquired with FLUOR/IOTA in a scanning mode. A short-stroke delay line sweeps through the zero optical path difference position at a speed which keeps the optical path difference rate almost constant and yields a fringe frequency of about 300 Hz. The length of each scan is of the order of 100 μm . Dark current sequences are recorded after each sequence and are used during the data reduction process for noise and signal calibration. Sequences are acquired every four seconds in regular turbulence conditions and a whole batch of observations comprises 100 sequences spreading over a few minutes.

We have used the method developed by Coudé du Foresto et al. (1997) to reduce the data and to derive the instantaneous

contrast of the fringe packets from each batch of observation of R Leonis as well as for its calibrators. The “instantaneous” transfer function of the instrument is computed from the fringe contrast measured on the calibrators. This computation and the computation of the final visibility estimates have been presented in Perrin et al. (1998).

The data have been collected using different baselines. The effective wavelength of the instrument is 2.15 μm . The 1996 observations were made with a single 16 m baseline. In 1997, the 11 m, 16 m, 21 m and 38 m baselines were used. Azimuths of the spatial frequencies common to the 1996 and 1997 observations are the same to within 10°. The range of azimuths covered by the 1997 observations is smaller than 30° because of the quasi North-South orientation of the L-shaped IOTA array. The data collected on R Leonis at IOTA during the two periods are listed in Table 1.

3. Diameter and intensity profile

3.1. Uniform disk diameter of R Leonis

The data of Table 1 are plotted on Fig. 1. Although the exact geometry of the stellar disk is *a priori* unknown, models based on radiative transfer computations for these extended objects are proposed in the literature (see Sect. 3.2). This section only deals with the simplest model of a stellar disk whose surface brightness distribution is uniform.

This model, although quite simple, is a good representation of the geometry of the star at low spatial frequencies. As a matter of fact, for spatial scales larger than one stellar radius, smaller details on the surface of stars are not visible. Spots and limb variations have a negligible contribution to the general geometry. As a consequence, the amplitude of the spatial frequencies of the stellar image are accurately described by the uniform disk visibility function for frequencies within the first null of this function.

Data points with spatial frequencies less than 40 cycles per arcsecond have been fitted by a uniform disk model for the two

¹ Infrared-Optical Telescope Array

² Fiber Linked Unit for Optical Recombination

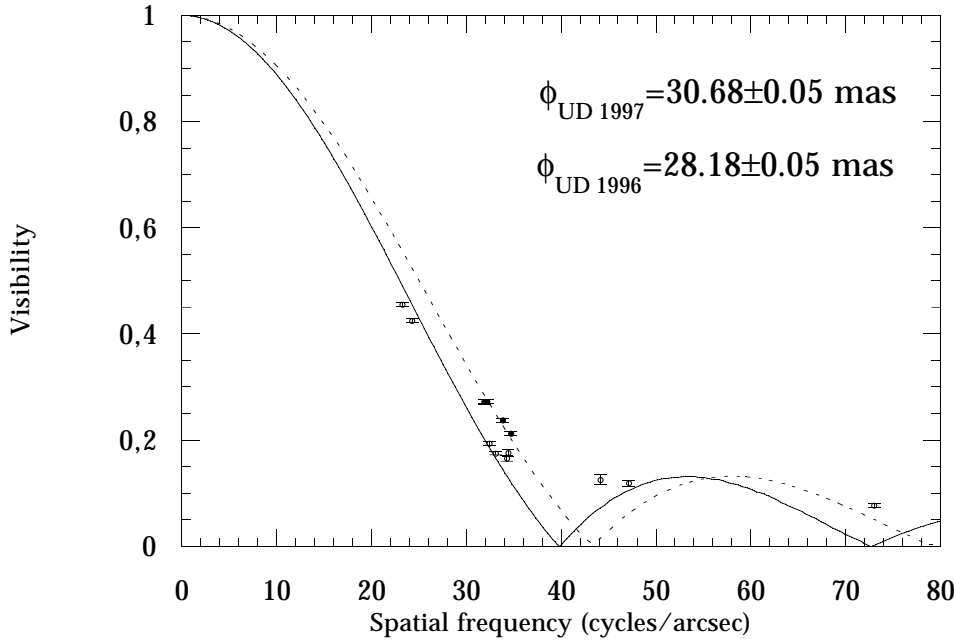


Fig. 1. Fit of the 1996 and 1997 data by uniform disk models. Full circles: 1996 data. Open circles: 1997 data.

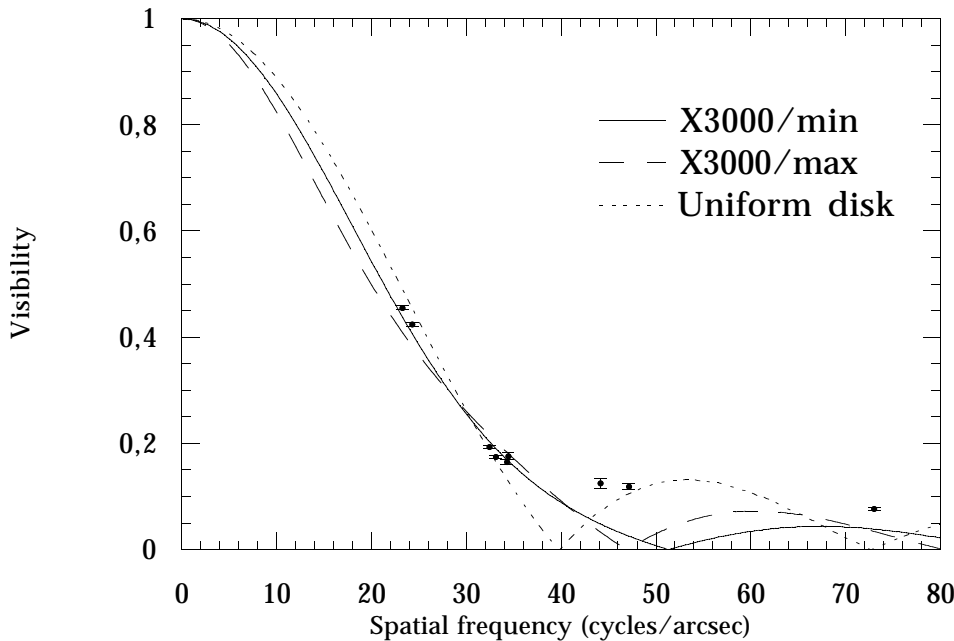


Fig. 2. Fit of the 1997 data by the X3000 Mira model. Continuous line: X3000/min model. Dashed line: X3000/max model. Dotted line: uniform disk model.

phases. The only parameter of this model is the apparent angular diameter of the star. For the two periods, the diameters yielding the smallest residuals of the fits are:

$$\phi_{UD,1996} = 28.18 \pm 0.05 \text{ mas} \quad (1)$$

$$\phi_{UD,1997} = 30.68 \pm 0.05 \text{ mas}.$$

These two estimates of the diameter of R Leonis in the K band can be compared with previous results obtained with different techniques and/or at different wavelengths. No K band diameter of R Leonis has been published as of today. Di Giacomo et al. (1991) have measured the star's diameter at phase 0.2 in the Br γ line of atomic hydrogen at $2.16 \mu\text{m}$ with

the lunar occultation technique. They have found that the occultation event is compatible with a disk $33 \pm 1.3 \text{ mas}$ in diameter. Despite the difference in bandwidth, this result is confirmed by our own findings since the whole K band measurement is a good approximation of the diameter of the photosphere of the star (see Scholz & Takeda (1987), hereafter ST) and Sect. 3.2). Some other measurements were made at visible wavelengths (see Sect. 1 for references) with interferometric techniques but are difficult to link to our results since the star appears larger because of light scattering and absorption by dust and molecules in higher layers. Nevertheless, the order of magnitude of photospheric diameters can be derived with the help of models and

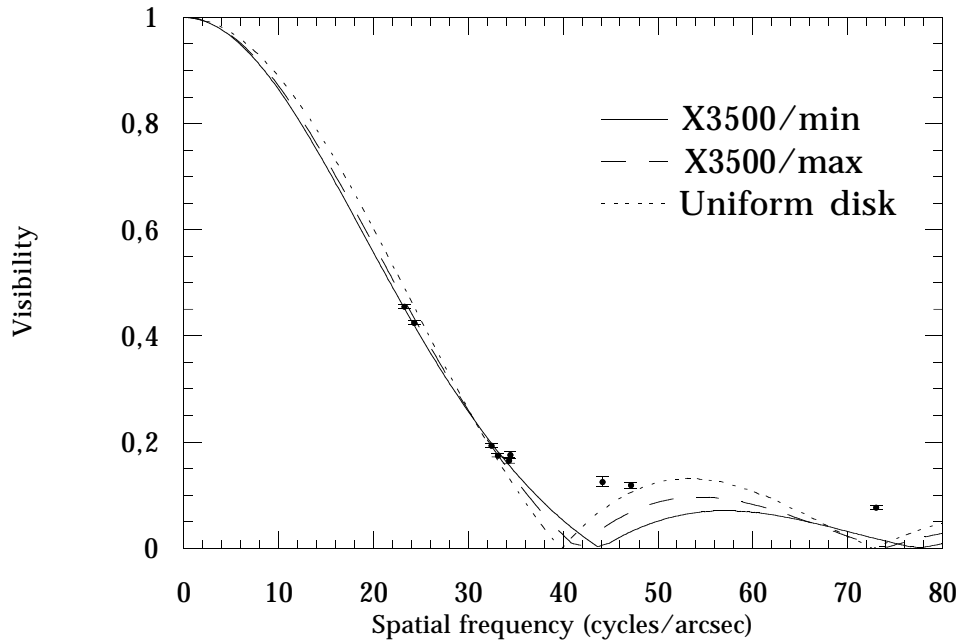


Fig. 3. Fit of the 1997 data by the X3500 Mira model. Continuous line: X3500/min model. Dashed line: X3500/max model. Dotted line: uniform disk model.

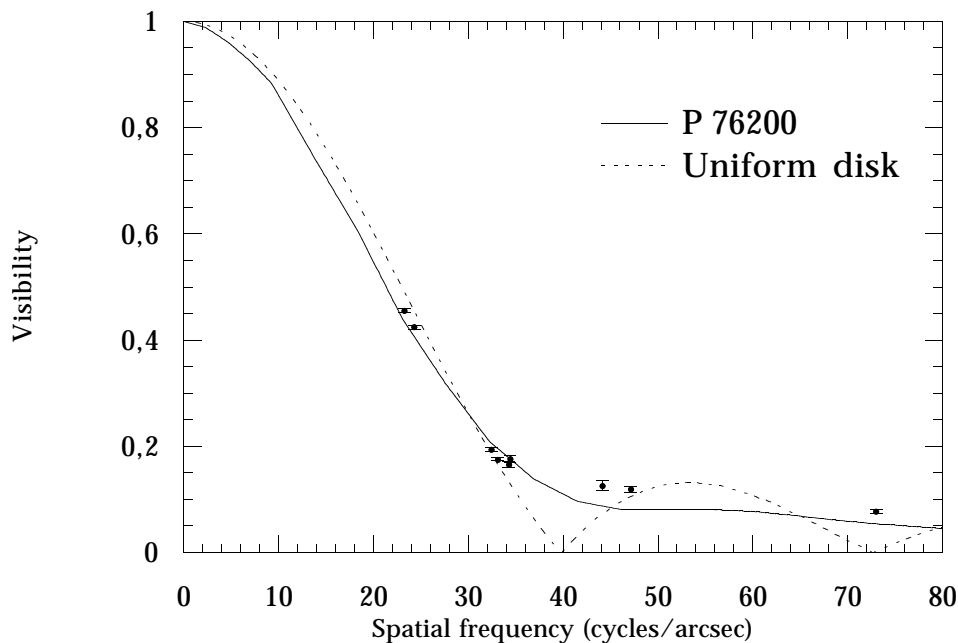


Fig. 4. Fit of the 1997 data by the P 76200 Mira model.

ranges between 37 and 61 mas (Haniff et al. (1995)). Although the lower value is compatible with our result, the higher value is almost twice as large. The photospheric diameters of 26.3 and 19.8 mas derived from observations at minimum phase at $11.15 \mu\text{m}$ (Danchi et al. (1994)) were obtained by modeling the dust emission and are therefore also model-dependent. They remain compatible with the K uniform disk diameters.

3.2. Limb darkened diameter

As Fig. 1 shows, high frequency visibility data are not compatible with uniform disk models. Photospheric radii derived from this model may not be an accurate approximation of the

real radii. The notion of photospheric radius is difficult to define for stars with an extended atmosphere. Following several authors (see Haniff et al. (1995)), the photosphere is defined as the layer at which the Rosseland mean optical depth is equal to one. Measurements of non-Mira M type giants in the K band yield limb-darkened diameters 2 or 3% larger than uniform disk diameters (Perrin et al. (1998)).

We have compared our data points for the two epochs first with the models published by ST and then with the more recent models by Hofmann et al. (1998) (hereafter HSW).

Two of the ST models are relevant in our case: the X3000 and X3500 models where the number after X is the effec-

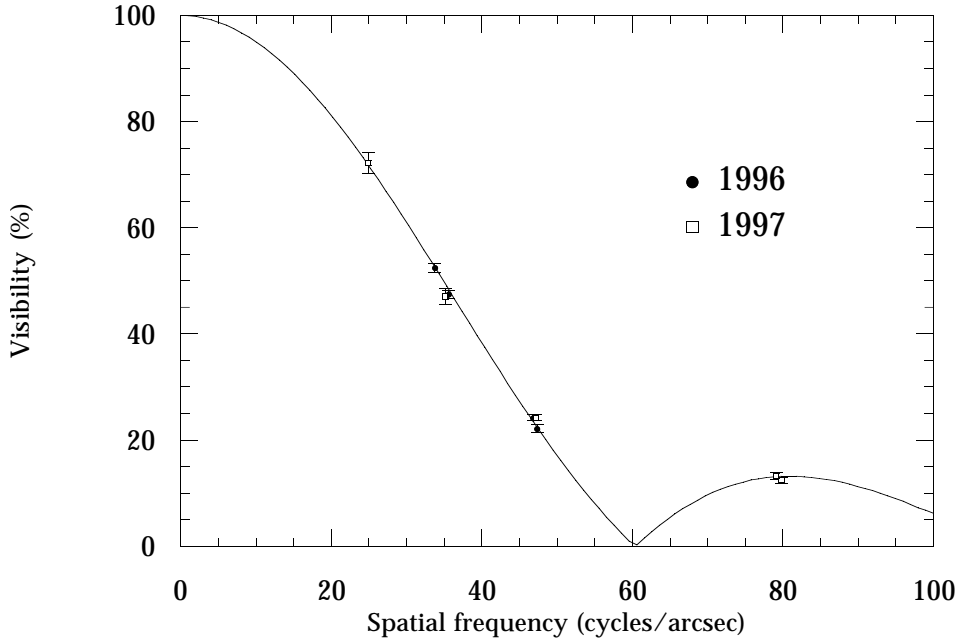


Fig. 5. Visibilities measured on α Bootis in 1996 and 1997. Full circles are the 1996 data points. Open squares are the 1997 data points. The continuous line is a uniform disk model fit of the 1996 data. The 1997 data points are fully consistent with the 1996 model and no variation of diameter is detected for this reference star.

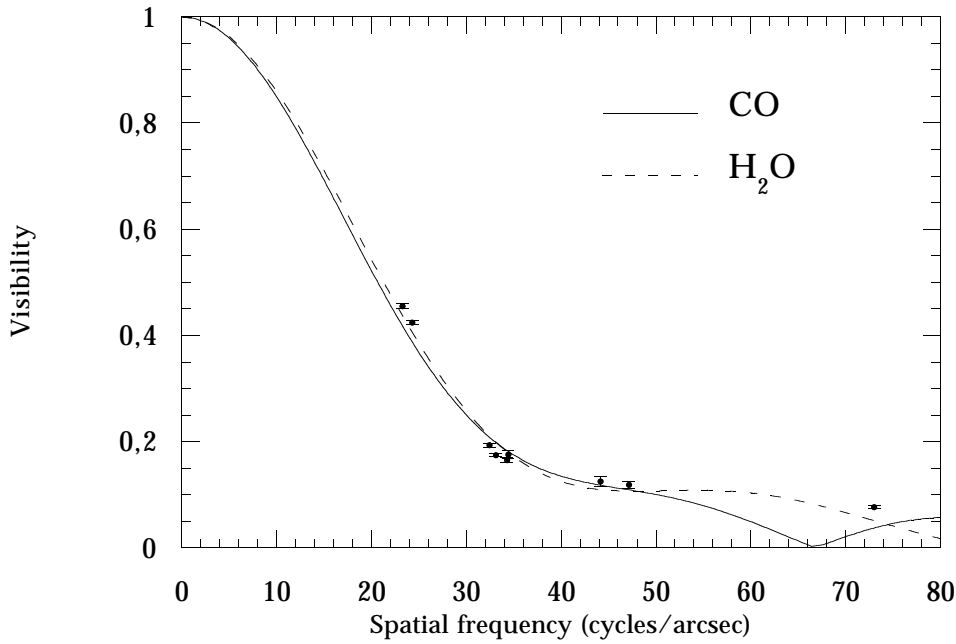


Fig. 6. Fit of the 1997 data by CO and H₂O intensity profiles of the X3000/max model.

Table 2. Fits of photospheric diameters by Mira models. UD is the uniform disk model. The X series are from Scholz & Takeda (1987) and the P 76200 model is from Hofmann et al. (1998).

Model	1996 Diameter	# points	$\chi^2/(\# - 1)$	1997 Diameter	# points	$\chi^2/(\# - 1)$
UD	28.18 ± 0.05	5	7.59	30.68 ± 0.05	6	40.9
X 3500/max	29.25 ± 0.06	5	3.92	31.85 ± 0.06	6	9.87
X 3500/min	29.67 ± 0.05	5	1.74	32.37 ± 0.06	6	4.63
X 3000/max	27.95 ± 0.08	5	2.54	30.21 ± 0.08	6	82.2
X 3000/min	29.21 ± 0.05	5	1.12	31.92 ± 0.05	6	16.4
P 76200	24.47 ± 0.06	5	1.01	26.61 ± 0.08	6	23.8

tive temperature of the parent static model of the photosphere (Bessell et al. (1989)). Intensity profiles are published in nine narrow bands at minimum and maximum luminosities. The photometric K band contains three of them centered on 2.00, 2.28 and 2.36 μm and corresponding, respectively, to H₂O bands, the continuum, CO and H₂O bands. We have mixed the three profiles by computing a composite mean weighted by a typical Mira-like spectrum and the supposed FLUOR spectral transmission. The composite profiles are Fourier transformed, assuming circular symmetry, to get composite visibility models. We have then fitted our data with these models. Once again, the fits to data with frequencies higher than 40 cycles/arcsecond are of poor quality. Examples of fits of the 1997 data are given in Figs. 2 and 3, corresponding to the X3000 and X3500 models respectively. Points with frequencies smaller than 40 cycles/arcsecond only have been taken into account. On each figure, we have plotted the best fits at minimum and maximum luminosity (continuous and dashed lines respectively). The dotted line is the best fit by a uniform disk model. The numerical results of these fits are given in Table 2. The diameters of the minimum light models have been properly scaled using the ratios between Rosseland radii for minimum and maximum light models given in Table 3 of ST. The reduced χ^2 of the fits (Columns 3 and 7) show that the fits with the Mira models generally yield better results than the fits by a uniform disk model. This is particularly true for the 1997 data. Visibilities have been measured at two different baselines and the fits are therefore sensitive to the curvature and to the slope of the models which are constrained, in first approximation, by the attenuation of the luminosity profile at the limb. The better quality of the fits by the X3500 models (at minimum and maximum light) is difficult to interpret since the effective temperature of the star is of the order of 2500 K at phase 0.2 (Di Giacomo et al. (1991)), which is better bracketed by the effective temperatures of the X3000/max and X3000/min models (3060 and 2280 K, respectively). This may be indicative of the work to be accomplished by theoreticians in this field to account for Mira surface luminosity profiles.

The same analysis has been accomplished with the HSW models. Six series of models have been computed with molecular opacities updated compared to those of ST. Pulsations are generated either by applying a piston to the upper atmospheric layers or more directly with self-pulsating atmosphere models. HSW have published a new set of conversion factors from uniform disk diameters to Rosseland diameters. We have selected those computed for phases closest to our observations. Most models display an average 5% difference between uniform disk and Rosseland diameters. These Rosseland diameters are compatible with the results of the fits by the ST models. Among the six series, some of the models from the P series lead to smaller radii by an amount that can be as large as 25%. We have fitted our data with one of the luminosity profiles that are presented in the paper with strong wing-like features (the P 76200 model from the P series at phase 0.5). The results of the fits are listed in Table 4 and the best fitting curve for the 1997 data is displayed on Fig. 4. The smaller diameters are the direct result of the wing-like structure of the stellar atmosphere. Yet, although

Table 3. Recently published linear radii for R Leonis.

R/R _⊙	Reference
495 ± 83	Tuthill et al. (1994)
444 ± 45	Haniff et al. (1995)
456 ± 59	van Leeuwen et al. (1997)
315 ± 84	this work, 1996
343 ± 91	this work, 1997

the wings lead to higher visibilities at the highest frequencies, there still remain some discrepancies between this model and the data. In Sect. 5, we will suggest and discuss some hypotheses on the origin of this difference. Besides, a closer look at the uniform disk to Rosseland diameter ratios for the entire set of the P models show that all ratios but two lie in the range 0.97–1.07 and that these ratios are cycle dependent. For example the 0.74 ratio occurs at phase 2+0 (using the notation of HSW) while it is 1.07 at phase 1+0, 1.06 at phase 3+0 and 0.99 at phase 4+0. This cycle-to-cycle dependence being impossible to connect to our observations it may be inappropriate to infer a smaller radius for the photosphere of R Leonis on the basis of the P 76200 model. But in any case, the wing-like structure of the luminosity profile needs to be given sufficient highlight in future studies to account for observations, as will be discussed in Sect. 5.

To remain consistent with the few lines before, and because the phases when R Leonis has been observed are intermediate between minimum and maximum light, we have chosen to keep the results of all fits with the ST models to compute the estimate of the Rosseland diameter in 1996 and 1997. The final diameters are the means of the four diameters of Table 2 at each epoch with error bars equal to the maximum errors quoted for each epoch. This yields:

$$\begin{aligned}\phi_{\text{Ross},1996} &= 29.02 \pm 0.08 \text{ mas} \\ \phi_{\text{Ross},1997} &= 31.59 \pm 0.08 \text{ mas.}\end{aligned}\quad (2)$$

3.3. Linear radius and pulsation mode

Given the above angular diameters, linear stellar radii can be derived from parallax data. The parallax of R Leonis has been determined by the Hipparcos mission to be $\pi_{\text{hip}} = 9.87 \pm 2.07$ mas (ESA (1997)). The linear radius of R Leonis in units of solar radii is then for the two periods:

$$\begin{aligned}R_{1996} &= 315 \pm 84 R_{\odot} \\ R_{1997} &= 343 \pm 91 R_{\odot}\end{aligned}\quad (3)$$

The nature of the pulsation of Miras is controversial. From their difficulty to produce realistic models of Miras pulsating in the first overtone, Bessell et al. (1996) conclude that long period Miras should pulsate in the fundamental mode. Depending on the mass of the central core, relations linking the period and the linear radius of Miras can be established (Wood (1990)). For

Table 4. Statistical analysis of results on uniform disk diameters. The last two columns are the reduced χ^2 of the fits obtained by assuming that the 1996 and 1997 data are fitted by a single diameter and two different diameters, respectively.

Star	$\phi_{UD,1996}$	$\phi_{UD,1997}$	$\chi^2_{1\phi,r}$	$\chi^2_{2\phi,r}$
α Boo	20.20 ± 0.08	19.99 ± 0.11	0.24	0.48
R Leo	28.18 ± 0.05	30.68 ± 0.05	13.26	5.38

a typical mass of the central core between $1 M_{\odot}$ and $1.5 M_{\odot}$ (Feast & Whitelock (1987)), these relations predict that a fundamental pulsator should have a radius between 220 and $270 R_{\odot}$ and that the radius of a first overtone pulsator should be in the range 340–450 R_{\odot} . Our linear radii are smaller than those of previous studies (see Table 3). In particular, the 1996 radius is clearly compatible with the two types of pulsators. This is partly due to the large error bar on the parallax estimate. We therefore conclude, on the basis of the diameters of Sect. 3.2, that the case of R Leonis is edgy and that no clear conclusion on its pulsation mode can be drawn based on the stellar radius criterion. But, we will show in Sect. 5 that including the high frequency data in the diameter computation may change this conclusion.

4. Variation with phase

R Leonis was observed during two runs in 1996 and 1997. Its average photometric period is 312.57 days (Kukarkin et al., 1971). Visual phases have been determined from AAVSO data (Mattei (1998)). They are given in Table 1. More exactly, the phases of the short frequency visibilities used to compute the diameters are 0.24 in 1996 and 0.28 in 1997.

4.1. Variation of the photospheric diameter with phase

The main result of Sect. 3 is that two different diameters have been measured for R Leonis in 1996 and 1997. The aim of this section is to establish the reality of the change of diameter of the photosphere of R Leonis during the period. We are going to show that, first, this change is not a geometrical artifact due to a possible asymmetric shape of the source and that, second, this change is not due to a variation of the response of the instrument.

The uniform disk diameter of R Leonis has been computed from visibilities measured at spatial frequencies smaller than 40 cycles/arcsec. These observations were carried out using the 11 m and 16 m baselines of IOTA, the latter baseline being common to the two runs. Azimuths of the 16 m frequency components are the same to within 10° . The variation of diameter cannot therefore be attributed to a confusion with the relative difference in size of 20% along two orthogonal axes detected by Lattanzi et al. (1997) with HST in the visible.

We have observed the K giant star α Bootis during the same runs in 1996 and 1997. This star is slightly variable and the variations may be explained by a pulsation process. Radial velocity measurements by Hatzes & Cochran (1994) reveal possible ra-

Table 5. Photometric observations of R Leonis from Whitelock et al. (1998). Errors on J, H and K are < 0.03 . Error on L is < 0.05 . The last column is the computed bolometric flux.

mean JD –2450000	J	H	K	L	F _{bol} ($10^{-13} \text{W cm}^{-2}$)
180	–1.47	–2.48	–2.92	–3.35	20.14 ± 2.48
503	–1.30	–2.34	–2.80	–3.27	17.57 ± 2.06

dial pulsations. A simple calculation shows that those pulsations may change the diameter of the star by less than 0.06% which is not detectable with FLUOR. α Bootis can therefore be used as a reference in this study. The uniform disk diameters of the two stars are given in Table 4 for the two epochs and the visibilities of α Bootis are plotted on Fig. 5. The two diameters of α Bootis measured in 1996 and 1997 are not significantly different. To perform a more precise study, we have analysed the data with two different simple models. In the first model, the diameter is constant with time whereas the second model uses two different diameters for the two epochs. The data are fitted with these two models and a reduced χ^2 is computed for each model. It is the residual of the fit divided by the number of data points minus the number of degrees of freedom of the model. Model 1 has one degree of freedom and Model 2 has two. The reduced χ^2 are given in Table 4. If the reduced χ^2 is smaller for the two diameter model then the uniform disk diameter variation is declared statistically significant between the two epochs. The results show that a variation is detected for R Leonis and that no significant variation is detected for the reference star α Bootis. This statistical analysis shows that the FLUOR measurements lead to stable diameter estimates for the non pulsating star and that the variation detected on R Leonis is a real fact.

4.2. Effective temperature variation with phase

The effective temperature of a star depends upon its angular diameter and its bolometric flux as can be deduced from the Stefan-Boltzmann law for black-body radiation. According to ST, the diameter has to be defined as the Rosseland diameter to get an accurate estimate of the temperature. In convenient units, the relation between effective temperature, bolometric flux and angular diameter can be written:

$$T_{\text{eff}} = 7400 \left(\frac{F_{\text{bol}}}{10^{-13} \text{W cm}^{-2}} \right)^{1/4} \left(\frac{1 \text{ mas}}{\varnothing_{\text{Ross}}} \right)^{1/2} \text{ K} \quad (4)$$

Quasi simultaneous photometric observations have been carried out at the South African Astronomical Observatory in the J, H, K and L bands, where most of the stellar flux is emitted (Whitelock et al. (1998)). These observations are reported in Table 5. The bolometric flux can be estimated from these infrared magnitudes by integrating the flux under the blackbody distribution which best fits the data. We have used the value of the extinction in the V band by Robertson & Feast (1981) ($A(V)=0.16$) and we have derived the extinctions in J, H, K and

L from the curves of Mathis (1990) where we have assumed that reddening is produced by interstellar diffuse matter. The values of the bolometric fluxes are given in the last column of Table 5.

Applying Eq. 4, we derive the effective temperatures for the two phases:

$$\begin{aligned} T_{\text{eff},1996} &= 2910 \pm 90 \text{ K} \\ T_{\text{eff},1997} &= 2696 \pm 79 \text{ K} \end{aligned} \quad (5)$$

The temperature difference between the two phases is 214 K, which is marginally significant compared to the error bars. We can nevertheless say that a decrease in effective temperature from phase 0.24 to phase 0.28 has been detected. The star cools down as it grows and releases energy. This decrease is compatible with theoretical studies (see e.g. Bessell et al. (1996)) and with other studies based on photometric data (Lockwood & Wing (1971)) or on interferometric data (van Belle et al. (1996)).

4.3. Other evidence of variability

We have shown that a geometrical change of R Leonis in the region of the photosphere has been detected. We are going to see how this compares to some other evidence of variability detected either with high angular resolution techniques or with spectroscopic observations.

The most recent observations of geometrical variability have been reported by Burns et al. (1998). These are based on measurements made with the COAST interferometer at visible wavelengths. These measurements are all the more complementary since some of them were performed at almost the same dates as ours to within a couple of weeks at most.

Burns et al. (1998)

find an average increase of uniform disk diameter of the order of 2% from phase 0.24 to phase 0.28. The absolute amplitude of the change may be indicative, but what is interesting from their cycle-to-cycle coverage of the photometric phases is that the strongest variation of diameter occurs at those phases close to 0.2. Merging the conclusions of the two studies, we find that the diameter of R Leonis increases after phase 0.2 in K and in visible bandpasses contaminated by TiO absorption bands. The Bessell et al. (1996) models predict that the Rosseland radius should decrease in this phase interval. In strong TiO absorption bands, the star radius may not repeat regularly with phase because it traces the motion of propagating shocks. For weaker and medium absorption bands, it should repeat more regularly and also decrease after phase 0.2. We therefore find a strong disagreement with model predictions. Burns et al. (1998) invoke a possible strengthening of the TiO bands during the photospheric cycles, but this cannot explain the K behaviour. As will be seen in the next section, absorptions may be larger than what is expected in the K band but it is doubtful that, for this range of wavelengths, the dynamic behaviour of the stellar radius can be changed by higher layers whose opacities are much lower than in the visible. Because the phase coverage of the K observations is low, it is impossible to guess whether the strong disagreement

with the models would happen at every photospheric cycle, but it is probably significant of a modeling difficulty.

Other observations collected on Mira itself in the visible have revealed temporal variations of the stellar size. Quirrenbach et al. (1992) found that their data set is compatible with a two component model with layers at different altitudes. Tuthill et al. (1995) found some large diameter variations (as large as 85%) with no correlation with photometric phase. These two observations show that the behaviour of Mira may be much different from that of R Leonis and that it is probably impossible to draw a direct comparison between the two stars except that of diameter variations.

The last evidence of variation that can be easily connected to our observations is from spectroscopic observations. Assuming that the variation of linear radius can be converted into motion of the photosphere between phase 0.24 and phase 0.28 we derive a speed of $18 \pm 4 \text{ km s}^{-1}$ (taking into account the uncertainty on parallax and diameters). Because of the small phase difference, this speed must be understood as an instantaneous one rather than an average one. Compared to the speed inferred by Hinkle (1978) from CO lines in the K band, our derivation yields a speed twice too large. This discrepancy may come from the fact that the occurrence of the maximum of R Leonis has an uncertainty of about ten days corresponding to an uncertainty on phases of 0.03. Given this uncertainty and the small difference in phases between our two observations, we may have an uncertainty of a factor of two on the speed of the photosphere (yielding a speed smaller by a factor of two). In this frame, our value is compatible with the spectroscopic observations, although rather inaccurate.

5. High frequency data

As we have seen in the previous sections, general models of Mira photospheres fail to reproduce the high frequency visibilities that we have measured with FLUOR. The difference is generally larger than 10%. This is much larger than the uncertainty of the measurements and this is therefore indicative of an extra structure which is not taken into account by the models. We have listed some tentative physical phenomena that are likely to occur in Miras and which may explain the excess of visibility:

1. limb brightening;
2. convective cells, spots;
3. diffusion.

5.1. Limb brightening

The spectrum of Mira stars comprises absorption but also emission lines that are produced by a shock heating process generated by the pulsations of the central core (Fox et al. (1984)). Most of these lines belong to the Balmer series in the visible part of the spectrum. Emission lines also appear in the K band region of the spectrum. Spectra reported by Hinkle & Barnes (1979) show Brackett- γ emission starting at phase 0.9 and disappearing after maximum luminosity at phase 0.1. Some other mechanisms can make some lines appear like emission lines (see

last paragraph of this section). For example, lines in the atmosphere of cool stars can be optically thick at the limb and appear in emission. Sasselov & Karovska (1994) have modeled this phenomenon to correct and interpret the diameter measurements of limb-brightened Cepheid stars by interferometric techniques, or to interpret microlensing events by Cepheids (Loeb & Sasselov (1995)). In their models, the center-to-limb distribution across the stellar disk in the continuum is classically limb-darkened, whereas in the Ca II $\lambda 8498$ emission line, the intensity is weak and flat across the disk and peaks at the limb.

In order to test the hypothesis of limb-brightening, we have made a simple model of an annular bright ring superimposed on a uniformly bright disk. We have neglected both limb-darkening of the parent disk and weak flat intensity inside the bright ring. The number of parameters of the model is thus reduced to four (diameter of the uniform disk (ϕ_*), internal radius of the ring (d), thickness of the ring (a) and ratio of the integrated surface brightness between the disk and the ring (I_*/I_{ring})) which is not too large a number if compared to the number of available data points in 1997. The parameters of the best adjustment are:

$$\begin{aligned}\phi_* &= 8.9 \pm 0.3 \text{ mas} \\ d &= 14.5 \pm 1.6 \text{ mas} \\ a &= 3.7 \pm 2.6 \text{ mas}\end{aligned}\quad (6)$$

$$I_*/I_{\text{ring}} = 1.22 \pm 0.1$$

The interpretation of the radii values by the limb-brightening model leads to the conclusion that these diameters are the ring diameter and that the diameter of the photosphere is overestimated by factor of three. Because this model may be too simple to be valid and since it is probably more physical to set better boundary conditions, we have run another fit by constraining the diameter of the photosphere and of the inner edge of the ring to be coincident. This model has the advantage of reducing the number of parameters to three (photospheric diameter, mean bright ring diameter and ratio of intensity). But it leads to a best solution for which the ring appears slightly darkened compared to the photosphere, the diameter of the ring being 23.3 mas. In those conditions, the model with a detached ring accounts better for the limb brightening assumption.

Coming back to the result of the first model, detected diameter changes of Sect. 4 could then be interpreted as ring extension changes due to the propagation of the shock front in the envelope of the Mira, the variation of the photosphere being probably smaller. Yet, in order to be valid, this hypothesis would require some support from spectroscopic observations bringing evidence of strong emission in the K band. We have not found any report of an emission of the level required by the I_*/I_{ring} ratio in the literature. We conclude that the physical basis of the limb-brightening model is not solid enough to explain the visibility excess at high spatial frequency.

5.2. Convection

A more classical explanation for high frequency visibility excess is the presence, at the surface of the Mira, of convection cells.

These may appear as hot spots whose individual size is a large fraction of the stellar disk. A few spots (not more than three) have been detected at the surface of a few late-type supergiants in the visible by Tuthill et al. (1997) and by Wilson et al. (1997). The order of magnitude of the size of these convective elements (hence their number) was predicted by Schwarzschild (1975).

Based on these observations and on the prediction, we can assume that a small number of convection cells may be present at the surface of R Leonis and produce our observed visibility excess. To keep the number of parameters reasonable (4) relative to the number of data points, we have compared our 1997 data to a model with one unresolved bright spot whose position and relative brightness are to be determined. The position has been constrained to be on the stellar disk. We can assume that it is not resolved by the instrument since it is a fraction of the stellar disk in size. When compared to this model, our data lead to the following best parameters for the star and the bright spot position and intensity:

$$\begin{aligned}\phi_* &= 21.2 \pm 0.2 \text{ mas} \\ \theta &= 103.1^\circ \pm 3.2^\circ \\ \rho &= 10.6 \pm 0.5 \text{ mas} \\ I_{\text{spot}}/I_* &= 0.13 \pm 0.34\end{aligned}\quad (7)$$

The spot is found to be exactly on the edge of the stellar disk. Because of the large spacing between our data points and their small number, the fitting algorithm tends to adjust the frequency of the wavy Fourier transform of the image of the unresolved spot (i.e. the distance of the spot to the center of the star) to minimize the contribution of the spot at low frequency and to maximize it at higher frequencies. This is a pure numerical effect. The only reliable conclusion that we may draw from this calculation is, firstly, that we need a better density of data points and, secondly, that, assuming that spots are present at the surface, more spots are necessary to build a model compatible with the data.

5.3. Diffusion

At visible wavelengths, long-period variable high resolution visibilities are well fitted by gaussian models (see e.g. Haniff et al. (1995)). The gaussian model accounts well for the flattening of the visibilities at high spatial frequencies due to light scattering by the envelope. Haniff et al. (1995) find a better agreement between their data and the gaussian model than with Mira atmosphere models, which they interpret to signify the difficulty of modeling the opacities of strong bandheads. This may be invoked in K for the CO and H₂O bands, although with weaker opacities and less scattering.

Let us assume that the H₂O and/or CO opacities are underestimated in Mira models. Then, the continuum luminosity profile differs from the one computed by ST. Multiple scattering of the continuum photons by the CO and H₂O envelope in the nearby molecular bands will make the continuum luminosity profile look like, in first approximation, the luminosity profile of the scattering medium. We have plotted the 1997 data with

the best fitting luminosity profiles in molecular bands of the X3000/max model in Fig. 6. Because of the smooth extension of the envelope, visibilities are flattened and drop down to zero more gradually. The Rosseland diameters for the CO and H₂O profiles are found to be:

$$\begin{aligned}\phi_{\text{CO}} &= 24.17 \pm 0.07 \text{ mas} \\ \phi_{\text{H}_2\text{O}} &= 18.09 \pm 0.05 \text{ mas}\end{aligned}\quad (8)$$

The K band luminosity profile would be a blend of the two profiles with a mean Rosseland diameter of the order of 22 mas. This luminosity profile better accounts for the observations than the X3000 model from ST and the P 76200 model from HSW. In this ad-hoc composite model, the scattering CO and H₂O molecules would be located in a shell 30 mas large, the characteristic size of the star as determined with a uniform disk model.

In order to give some support to this hypothesis, some independent evidence of strong scattering by molecular species is required. The very deep molecular CO and (at times) H₂O absorption seen in the K band of R Leo are probably indicative of scattering opacity, since the lines are much deeper than can be readily accounted for with a thermal source function. The depth of the lines contributing to the strong line blanketing throughout this region is difficult to estimate, due to uncertainties about the continuum level, even at high spectral resolution. In sum, it appears that scattering opacity throughout the K band is possible, but the spectroscopic evidence is merely suggestive. Spectral studies of CO and H₂O lines of R Leonis have been published in the late seventies (Hinkle (1978), Hinkle & Barnes (1979)). It was shown that the lines originate from two components. A warm component which is close to the stellar photosphere and a cooler component located at the inner edge of the circumstellar shell with an excitation temperature of the order of 1000 K. The cool component dominates the molecular lines in the K band. Some of the CO lines display deep absorption exceeding the half continuum level at phase 0.2. For H₂O, no such strong absorption is reported, yet it is underlined that continuum placement is a problem especially near maximum light.

As a consequence, the hypothesis of scattering by molecular species in the K band may at least partly explain the high frequency points that we have measured. This simple approach remains a first attempt to explain our observations. Some further modeling is necessary to provide a more complete explanation, the above rationale being a first step in the investigation.

5.4. Discussion

It turns out from the above analysis that any inclusion of an extra feature in the modeling of R Leonis tends to decrease the stellar diameter by a large amount (of the order of 25%). Among the three scenarios suggested, the scattering hypothesis seems to be the most encouraging. The limb brightening hypothesis may be the least probable since it requires strong emission lines that have never been detected in the K band. Besides, imposing boundary conditions to the simple model leads to limb darkening and to the negation of the assumption.

In reality R Leonis is probably a blend of limb darkening, scattering and spots indicating that the Rosseland diameter may be smaller than what can be guessed from usual models. Therefore, the angular diameter of the photosphere may have been closer to 24 mas in 1997 than to 31.59 mas. Applying this scaling factor to the 1996 diameter leads to a 22 mas diameter.

This would of course have implications on the fundamental parameters of this Mira-type star. The mean photosphere linear radius would be of the order of 250 solar radii and R Leonis would therefore pulsate in the fundamental mode as often claimed by theoreticians, thus clarifying the conclusions of Sect. 3.3. The other consequence is that the effective stellar temperature would be larger with $T_{\text{eff}} \simeq 3300$ K in 1996 and $T_{\text{eff}} \simeq 3070$ K in 1997. The spectral type of R Leonis determined by Lockwood & Wing (1971) for the same phases is M 7.0–7.5 which, for non-Mira giants, corresponds to effective temperatures of the order of 3100 K (Perrin et al. (1998)). The revised temperatures are thus more consistent with the spectral type of less luminous giants.

5.5. Enhanced scale height

In an extended atmosphere such as exists in R Leo, the so-called limb darkening effect consists of two parts. One part is the conventional limb darkening, observed for example in the sun, whereby the surface brightness of the star decreases at the limb due to the decrease of temperature with height in the stellar atmosphere, and which occurs even in an atmosphere of negligible thickness, when the stellar diameter is virtually independent of wavelength. The second part arises due to the fact that at different wavelengths, a greatly extended atmosphere does in fact have a wavelength dependent shape and diameter. This component of the brightness distribution depends sensitively on the scale height in the model, and hence on the detailed physics of the pulsation computations. Any effects which increase the actual scale height over the model scale height would similarly tend to extend the brightness profile drop over a larger radius, effectively smearing the limb profile.

This also suggests that the angular diameter observed in high excitation lines will be characteristic of a deep, high temperature layer, and the angular diameter observed in low excitation lines will be characteristic of a low excitation layer. Distinguishing between these observationally will give direct access to the scale height, a parameter not otherwise accessible. Though less direct, the smearing of the stellar limb profile observed already begins to constrain the model, though currently through the haze of other issues mentioned above.

It would be reasonable to expect the effective temperature computed from a representative angular diameter to be intermediate between the temperature extremes observed spectroscopically. The extremes in the photospheric region, from CO excitation in the pulsating layer, are 3000 and 4500 with a temperature of about 3300 K at phases 0.24 and 0.28 (Hinkle et al. (1984)). The deduced T_{eff} of 3000–3300 satisfies this criterion of reasonableness.

6. Future observations

It is clear from what has been discussed so far that some other observations are necessary and that these new data raise as more questions than they can answer. Based on our conclusions, we therefore recommend some complementary observations that may help solve some of these new questions.

First, a wider sample of observations are necessary to cover a full cycle of photometric variability and to study possible non periodic effects. The precision of our data would allow an accurate diameter to phase variation determination along with the evolution of the effective temperature of the object. Second, a better coverage of the plane of spatial frequencies (especially in azimuth) would give access to possible asymmetries and would allow a better diagnostic of the presence of features at the surface of the star. Third, increasing the spectral resolution of the interferometric observations would certainly help build connections between the structures identified in the image and some of the species synthesized by the star. The easiest action would be to use narrower filters to separate the continuum from the absorption bands. Eventually, both a spectroscopic and a photometric follow-up of the interferometric observations will allow a better understanding of the observations, which at this stage is mandatory to achieve a realistic modeling of the sources and reach an understanding of the physical phenomena they represent.

7. Conclusion

We have reported the first direct detection of the variation of the size of the photosphere of R Leonis from phase 0.24 to phase 0.28 generated by the pulsation of the star. Comparison with a uniform disk model yields a photospheric radius intermediate between that of fundamental and first overtone pulsators. High spatial frequency data acquired in 1997 display an excess of visibility that we interpret as the possible signature of scattering by molecular species in the atmosphere. A direct effect of scattering on models is to yield lower values for the photospheric radius to 22 and 24 mas which make R Leonis a fundamental pulsator. We have found a disagreement with dynamical models of Miras which predict that the diameter of the photosphere should decrease after phase 0.2. The same disagreement holds for recent measurements with the COAST interferometer in the visible.

Some more observations are required in the future and should combine high angular resolution with spectroscopy and photometry. These new results show how important calibration issues are in astronomical interferometry to permit valuable tests of models. The new generation instruments will certainly benefit from accurate beam combiners and will bring new and better understanding to the physics of Mira variables, and, of course, many other types of sources.

The authors would like to salute the memory of their friend and colleague Jean-Marie Mariotti who died tragically in July 1998. He was the initiator of the fiber interferometer and actively contributed to its realization and success. This paper is dedicated to him.

Acknowledgements. The authors would like to thank the referee for his valuable comments.

References

- Bessell M.S., Scholz M., Wood P.R., 1996, *A&A* 307, 481
 Bessell M.S., Brett J.M., Scholz M., Wood P.R., 1989, *A&A* 213, 209
 Burns D., Baldwin J.E., Boysen R.C., et al., 1998, *MNRAS* 297, 462
 Carleton N.P., Traub W.A., Lacasse M.G., et al., 1994, *Proc. SPIE* 2200, 152
 Coudé du Foresto V., Ridgway S.T., Mariotti J.-M., 1997, *A&AS* 121, 379
 Coudé du Foresto V., Perrin G., Ruilier C., et al., 1998, *Proc. SPIE* 3350, 856
 Danchi W.C., Bester M., Degiacomi C.G., Greenhill L.J., Townes C.H., 1994, *AJ* 107(4), 1469
 Di Giacomo A., Richichi A., Lisi F., Calamai G., 1991, *A&A* 249, 397
 Dyck H.M., Benson J.A., Carleton N.P., et al., 1995, *AJ* 109 (1), 378
 ESA, 1997, *The Hipparcos Catalogue*, ESA SP-1200
 Feast M.W., Whitelock P.A., 1987, In: Kwok S., Pottasch S.R. (eds.) *Late stages of stellar evolution*. Reidel, Dordrecht, 33
 Fox M.W., Wood P.R., Dopita M.A., 1984, *ApJ* 286, 337
 Haniff C.A., Scholz M., Tuthill P.G., 1995, *MNRAS* 276, 640
 Hatzes A.P., Cochran W.D., 1994, *ApJ* 422, 366
 Heske A., 1990, *A&A* 229, 494
 Hinkle K.H., 1978, *ApJ* 220, 210
 Hinkle K.H., Barnes T.G., 1979, *ApJ* 234, 548
 Hinkle K.H., Scharlach W.W.G., Hall D.N.B., 1984, *ApJS* 56, 1
 Hofmann K.-H., Scholz M., Wood P.R., 1998, *A&A* 339, 846
 Kukarkin B.V., Kholopov P.N., Pskovsky Y.P., et al., 1971, *General Catalog of Variable Stars 3rd edition*
 Labeyrie A., Koechlin L., Bonneau D., et al., 1977, *ApJ* 218, L75
 Lattanzi M.G., Munari U., Whitelock P.A., Feast M.W., 1997, *ApJ* 485, 328
 Lockwood G.W., Wing R.F., 1971, *ApJ* 169, 63
 Loeb A., Sasselov D.D., 1995, *ApJ* 449, L33
 Mathis J.S., 1990, *ARA&A* 28, 37
 Mattei J.A., 1998, *Observations from the AAVSO International Database*, private communication
 Perrin G., Coudé du Foresto V., Ridgway S.T., et al., 1996a, In: Eiroa C., et al. (eds.) *Infrared Space Interferometry Workshop*, Toledo, 233–239
 Perrin G., Coudé du Foresto V., Ridgway S.T., et al., 1996b, In: Paresce F. (ed.) *Science with the VLT Interferometer*. Garching, 318–325
 Perrin G., Coudé du Foresto V., Ridgway S.T., et al., 1998, *A&A* 331, 619
 Quirrenbach A., Mozurkewich D., Armstrong J.T., et al., 1992, *A&A* 259, L19
 Robertson B.S.C., Feast M.W., 1981, *MNRAS* 196, 111
 Sasselov D.D., Karovska M., 1994, *ApJ* 432, 367
 Scholz M., Takeda Y., 1987, *A&A* 186, 200
 Schwarzschild M., 1975, *ApJ* 195, 137
 Traub W.A., 1998, *SPIE* 3350, 848
 Tuthill P.G., Haniff C.A., Baldwin J.E., 1997, *MNRAS* 285, 529
 Tuthill P.G., Haniff C.A., Baldwin J.E., 1995, *MNRAS* 277, 1541
 Tuthill P.G., Haniff C.A., Baldwin J.E., Feast M.W., 1994, *MNRAS* 266, 745
 van Belle G.T., Dyck H.M., Benson J.A., Lacasse M.G., 1996, *AJ* 112, 2147

- van Leeuwen F., Feast M.W., Whitelock P.A., Yudin B., 1997, MNRAS 287, 955
- Whitelock P.A., et al., 1999, in preparation
- Wilson R.W., Dhillon V.S., Haniff C.A., 1997, MNRAS 291, 819
- Wood P.R., 1990, In: Mennessier M.O., Omont A. (eds.) From Miras to planetary nebulae: which path for stellar evolution? Editions Frontières, Gif-sur-Yvette, 67